Kathmandu University
Journal of Science, Engineering and Technology

Giri *et. al.*, Vol. 13, No. I, October 2017, pp 20-35.

ORIGINAL RESEARCH ARTICLE OPEN ACCESS

PERFORMANCE ANALYSIS OF MICROCONTROLLER BASED ELECTRONIC LOAD CONTROLLER

Amir Raj Giri *, Bikesh Shrestha, Rakesh Sinha
Department of Electrical and Electronics Engineering, Kathmandu University, Dhulikhel, Nepal

*Corresponding author's email: amir.giri@student.ku.edu.np
Received 14 December, 2015; Revised 19 January, 2016

ABSTRACT
The paper 'Performance Analysis of Microcontroller based Electronic Load Controller' is an approach for design, fabrication and performance analysis of microcontroller based ELC for 300 Watt Pico hydro controller. Electronic Load Controller (ELC) is an approach for regulating total power in the system with Pico-hydro power plant. The paper presents a unique method to maintain the system performance by regulating the generated power. The system voltage and current is measured by microcontroller to calculate the consumer power. Based upon the consumer power the dump power is varied accordingly. The performance analysis of ELC unit was done with power source from Nepal Electricity Authority (NEA) grid line as well as with separately excited induction generator under various loading conditions. The different resistive, capacitive and inductive loads were taken into consideration and the performance of the system based on voltage, current and power profiles were obtained.

Keywords: Load control, microcontroller, induction generator, voltage measurement, current measurement

INTRODUCTION
Electronic load controller (ELC) is an approach for regulating dump power with micro-hydro as power source. The ELC maintains the fixed frequency in the system with the control of power to the dump load. [1]. This particular ELC developed takes a different approach towards the load control mechanism. Usual available ELCs in the commercial market measure either frequency or voltage to control the system. The paper presented is based on the power measurement at the consumer side so as to maintain the power across the dump load. Due to high cost of governor system to be implemented in Pico-hydro the ELC provides a cheap and robust system for power control. If the consumer power used is lower than the generated amount the remaining power is supplied to the dump load through the ELC. The concept is well described by the figure 1.

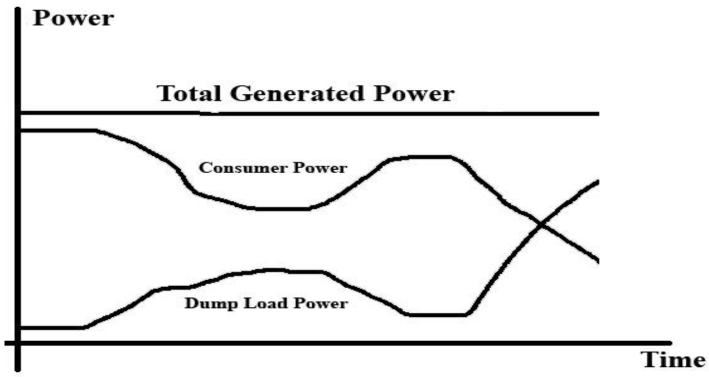

Figure 1. Consumer Power and Dump Load Power relation in ELC System

Giri *et. al.*, Vol. 13, No. I, October 2017, pp 20-35.

Figure 1, shows the ELC concept to maintain the total power constant at the generator terminals. This is done by changing the power to the dump load with the variation of the consumer power. The microcontroller senses the power at the consumer end and then provides the required firing angle to the triac to dump the excess power. Comparing with the commercially available ELCs, the microcontroller based ELC reduces the number of components that are required to build one. Along with that it reduces the cost which makes ELC board cheaper to manufacture. As it is microcontroller based with few components it is easy to build, easily upgradable and easy to debug if any.

BACKGROUND

Many research and designs has been done with ELC in the past. The new designs are created from time and again by various authors with increasing reliability, robustness and cost effectiveness. In July 1984, Kormilo and Robinson described the role of electronic load controllers in reducing the cost of small hydro schemes with particular reference to the situation in Papua New Guinea. A prototype controller based on an AIM 65 microcomputer is described [2].

In December 2006, Singh and Kasal described the analysis and design of voltage and frequency controllers for asynchronous generators to be used in isolated constant power applications such as Pico and micro hydro sites [3]. These controllers are basically load controllers which maintain the load power at generator terminals which in turns maintain the system frequency constant. A set of load controllers are designed, modeled and simulated in Matlab using Simulink and PSB (Power System Block-set) toolboxes to demonstrate their performance.

In November 2003, Gurung and Freere investigated the influence of excitation capacitors on the power output and efficiency of a 4 pole, 3 phase self-excited squirrel cage induction generator running at 1500 rpm and feeding a single phase resistive load at 220v output [4]. The comparative study of different capacitor configuration and sizes on the generator performance was the main area of interest. They achieved a maximum efficiency of 67% as a single phase output from three phase induction generator.

In 2013, Roodsari, Nowiki and Freere described a new concept of distributed electronic load controller for voltage regulation in micro hydro systems with transfer of excess power to households [1]. Instead of dumping excess power at the generating station itself on heaters the authors proposed a new concept of decentralizing the excess power to each and every household. Each household would be allocated certain power and the excess power from each household would be used on the same house as water heater.

The ELC available in the common market are commonly designed with the analog circuits. This makes the ELC board bulky and during problem occurrence the troubleshooting process becomes very complicated. The paper describes a new approach towards the development of ELC and its performance analysis with various loads. The Microcontroller based ELC presented here has high accuracy, robustness and most important of all; cost effectiveness. The circuitry is reduced to great extent comparing with presently available ELC. This makes it easy to troubleshoot problems (if any). The use of microcontroller further could enable the ELC to perform various additional functions such as data logger, live data transmission to monitoring stations and much more.

Giri *et. al.*, Vol. 13, No. I, October 2017, pp 20-35.

A. Phase Angle Control

Phase angle control is a method of power limiting with the help of power electronic devices such as Thyristors and TRIACs where the gate signals of these devices are controlled by a PWM signal. The duty cycle variation of the PWM signal varies the phase angle control of the AC voltage. This control of the voltage in turn limits the power through the device [5].

B. Precision Rectification and Peak Detection

The precision rectifier, also known as a super diode, is a configuration obtained with an operational amplifier in order to have a circuit behave like an ideal diode and rectifier. It is useful for high-precision signal processing where the amplitude of the input signal is very small.

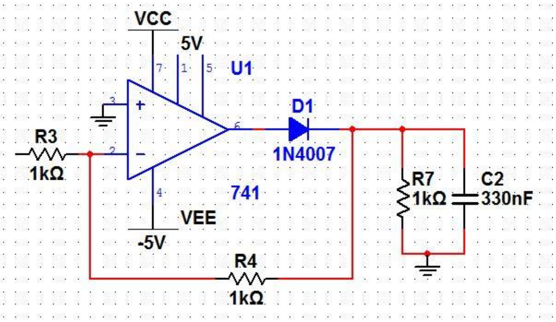

Figure 2. Precision Rectification and Peak Detection Circuit

Figure 2, shows a basic precision rectification and peak detection circuit. This circuit acts as a signal conditioner to the microcontroller and maintains the signal level to the acceptable limit to the input of the microcontroller.

C. Single Phase Output from Three Phase Self Excited Generator

The ELC is tested with single phase power input from the induction machine. An induction machine can be used as stand-alone generator when capacitors are connected over its terminals [6]. Standard three-phase induction motors can be used and these are cheap, rugged and require little maintenance., The capacitors connection in ‘C-2C’ arrangement helps to maintain the stable condition during unbalanced loading for single phase output [4]. The ‘C-2C’ arrangement is shown in the figure 3.

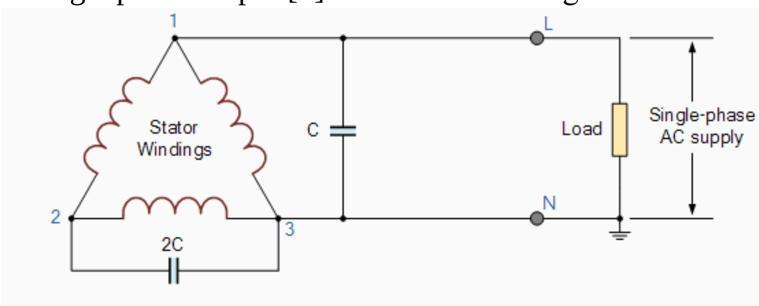

Figure 3. C-2C Connection Diagram for Single Phase Output

Figure 3, shows the configuration diagram used across the three phase generator to obtain a single phase supply. This configuration has the efficiency of about 65% [4].

Kathmandu University
Journal of Science, Engineering and Technology

Giri *et. al.*, Vol. 13, No. I, October 2017, pp 20-35.

SYSTEM ANALYSIS AND EXPERIMENT

A. Voltage Measurement

A step-down transformer of size (12-0-12) was used to step down the voltage. The resistor network was used to step-down to the voltage (2.5V) further before giving input to the signal conditioner. The precision rectification and peak detection was then carried out. The signal is then given to the ADC of Micro-controller. This signal is fed to the ADC of the microcontroller. The input RMS voltage value is obtained with multiplication of the voltage at signal conditioner and the ratio of the voltage divider. The actual RMS voltage from the grid is thus calculated. The voltage measurement circuit is presented in the figure 4.

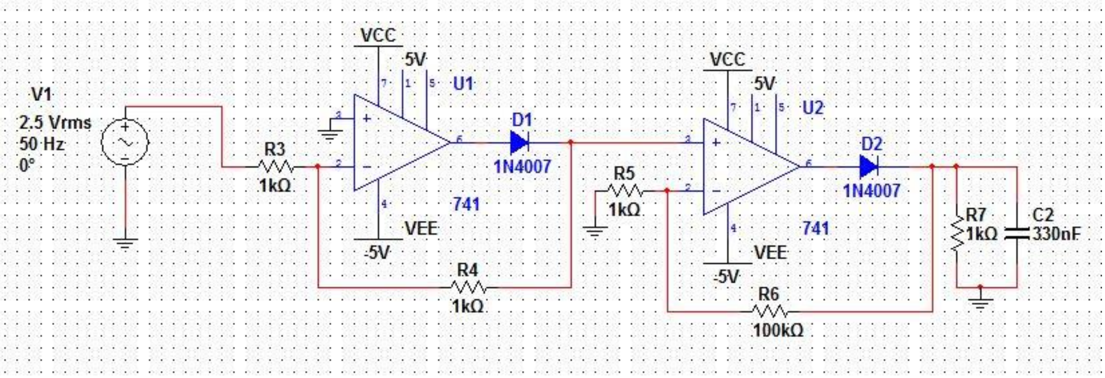

Figure 4. Voltage Measurement Circuit with Precision based Peak Detector

Figure 4, shows the circuit diagram of the voltage measurement circuit. This circuit is a precision based peak detector. The current measurement also uses the identical circuit. The value of the measured voltage varied within some range. For a 220V input voltage the measured voltage range was:

Max. Voltage = 222.57 V
Min. Voltage = 217.2 V
Range= Max – Min = 5.37 V

$$\text{Error Percentage} = \frac{\text{Max}-\text{Min}}{220} * 100$$
$$= 2.4409\ \%$$

Here, the error percentage in measuring the voltage was 2.44%.

B. Current Measurement

The current of the consumer side was measured using Current transformer. The current induces the voltage across the secondary terminal which was further signal conditioned and precision rectification was done. The signal is then given to the ADC of Micro-Controller. The input RMS current value is obtained with multiplication of the voltage at signal conditioner and the ratio of the CT. The actual RMS current in the consumer side is thus calculated.

The value of the measured current varied within some range. For a 1.19 A input current the measured current range was:

Max. Current = 1.2 A

Giri *et. al.*, Vol. 13, No. I, October 2017, pp 20-35.

Min. Current = 1.18 A
Range= Max – Min = 0.02 A

Error Percentage $= \frac{Max-Min}{1.19} * 100$

$=1.6806\ \%$

Here, the error percentage in measuring the current was 1.68%.

C. Power Calculation

The power is calculated through the values obtained from the Current Transformer (CT) and potential dividers at the microcontroller. The signal conditioner circuit is placed between the microcontroller and the input sensors. The voltage and the current values are calculated by the microcontroller. The product of the voltage and current gives the power across the consumer side.

Here,

Apparent Power, (S) = Voltage * Current

The power that is measured by microcontroller is apparent power with unit VA. The measurement of the apparent power accounts for both the active and reactive power supplied by the system. This makes the system ideal for the low power factor operations. The calculated power helps to determine the firing angle of the TRIAC. The firing angle controls the amount of power to be diverted to the dump load.

Error in Power Measurement = Error in Voltage + Error in Current
=2.4409% +1.6806%
=4.1215%

Thus the measured power from the microcontroller has an error of 4.1215 %.

D. Zero Cross Detector

The zero cross detection of the input signal is done with the help of signal conditioner resistors and the Op-Amp. The zero cross signal is the square wave with the rising and falling edge as the interrupt signal. The TRIAC operation is based upon this zero cross signal. The MULSTSIM circuit is presented in the figure 5.

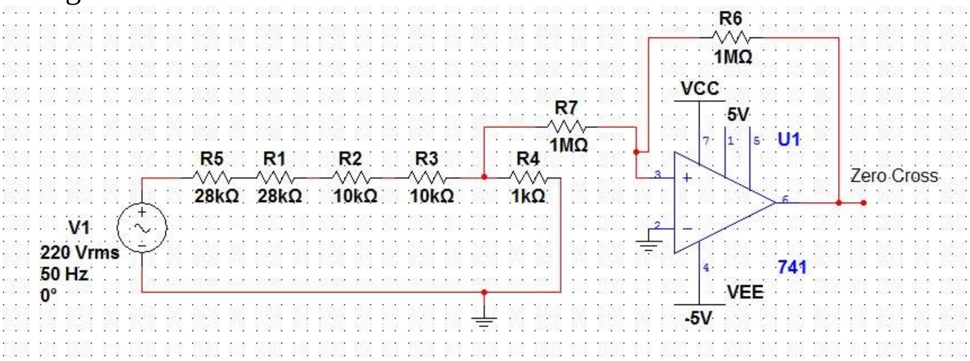

Figure 5. Zero Cross Detection Circuit Simulation in MULTISIM

Kathmandu University
Journal of Science, Engineering and Technology

Giri *et. al.*, Vol. 13, No. I, October 2017, pp 20-35.

E. Control of Dump Load

The power to be diverted to the dump load was controlled through the TRIAC. The variation of the firing angle resulted in the variation of the output power to the dump load. The firing angle was provided to the TRIAC on the basis of time delay. E.g. for a 50 Hz signal the time period is 20ms.So to achieve the firing angle of 90° the delay time is 5ms from the zero cross signal. The graph of the firing angle delay with respect to the power output is presented in the figure 6.

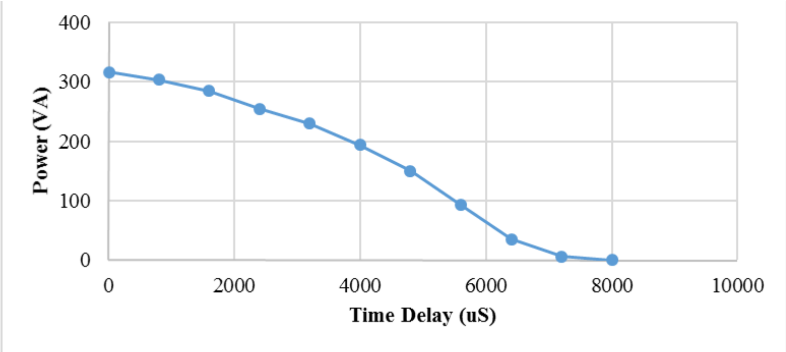

Figure 6. Graph of Power vs Firing Delay

Figure 6, shows the inverse relation between the power and the firing delay. The value obtained from the relation between the power and time delay is linearized and the linear relation is used to control the excess power. The power at the consumer load is calculated through the microcontroller and then the required power is dumped with the linear relation between the power and delay timing.

METHODOLOGY

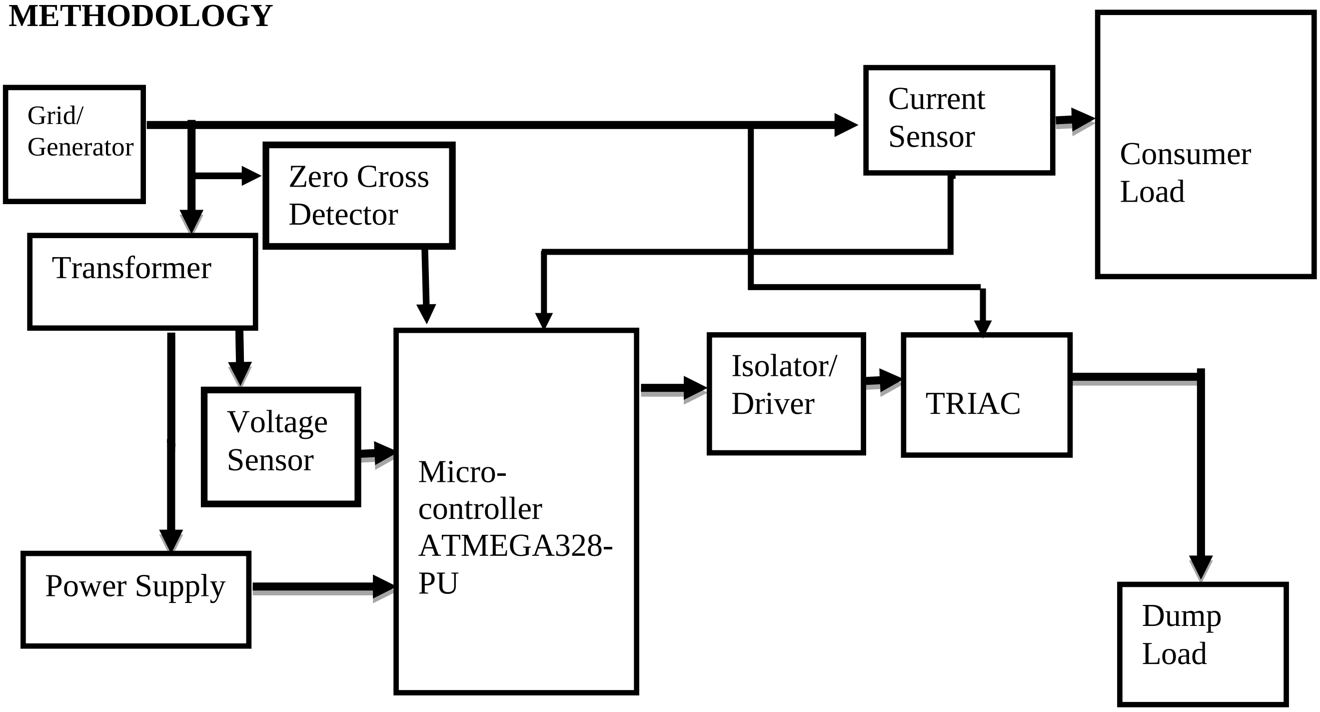

Figure 7. Components of Microcontroller based ELC

Giri *et. al.*, Vol. 13, No. I, October 2017, pp 20-35.

Figure 7, shows the general components of the ELC unit. The generated voltage is stepped down using step-down transformer (12-0-12). The stepped down voltage is used in powering the microcontroller (ATMEGA328) and sensing the line voltage of the generated voltage through the potential divider. The zero cross detector (LM741) is used to detect the zero crossing points of the input voltage which is fed to the microcontroller. The CT is used to measure the current in the household with the microcontroller. The power is calculated in VA and compared with the reference power (300 VA). Ground isolation and gate driving is done between TRIAC and microcontroller with opto-coupler (MOC3011). The microcontroller generates the firing signal based on measured power and the zero cross detection. The hardware circuit of the ELC board is shown in the figure 8.

Figure 8. ELC Board with Voltage and Current Inputs and Triac Control

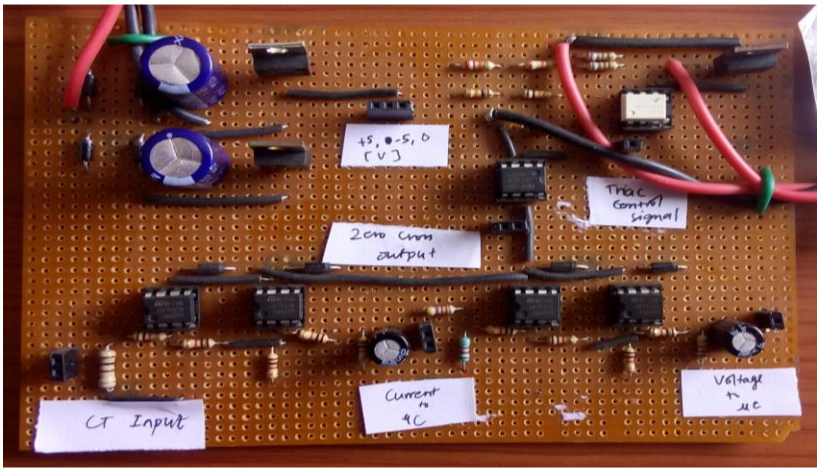

Figure 9. Experimental Hardware Setup of Microcontroller based ELC

Giri *et. al.*, Vol. 13, No. I, October 2017, pp 20-35.

Figure 9, shows the hardware setup of experimentation in the power lab. The DC motor was used as prime mover and an Induction Generator was used as power source. The various resistive, inductive and capacitive loads were used for the performance analysis. Wattmeter was used to read the voltage, current and power profile. Oscilloscope was used to observe the various waveforms across the dump load.

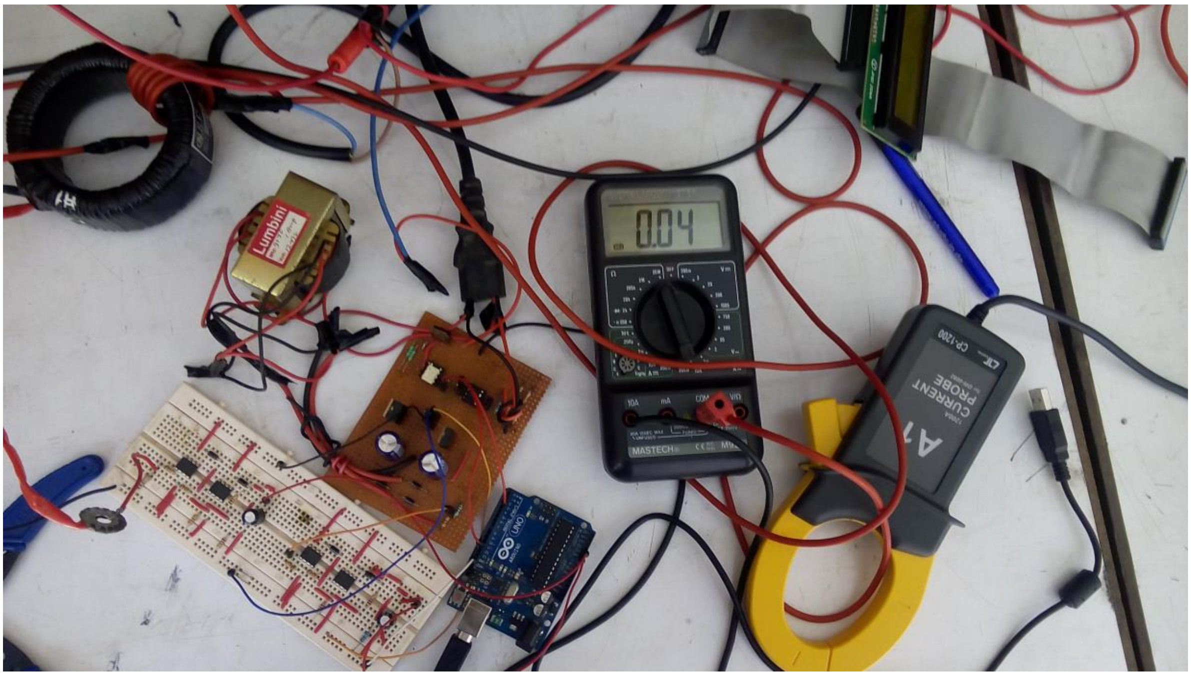

Figure 10. Measurement and Control Block of ELC

Figure 10, shows the measurement block of current and voltage. The value obtained with CT is cross checked with the Ammeter reading. The ATMEGA328 microcontroller is used to control the firing angle of the ELC.

A. Triac Control Mechanism

First, the current and the voltage of the consumer side is measured by the micro-controller. Then, the power consumed is calculated. If power is in the defined range i.e. 295-305 then the micro-controller just reads the current and voltage value and maintains the same firing angle. If the power is greater than 305 then the dump power is set zero. If power is less than 305 then the firing angle is calculated so the power required to maintain fixed power is diverted through TRIAC to the dump load. Figure 11 shows the triac control mechanism of the ELC.

Kathmandu University
Journal of Science, Engineering and Technology

Giri *et. al.*, Vol. 13, No. I, October 2017, pp 20-35.

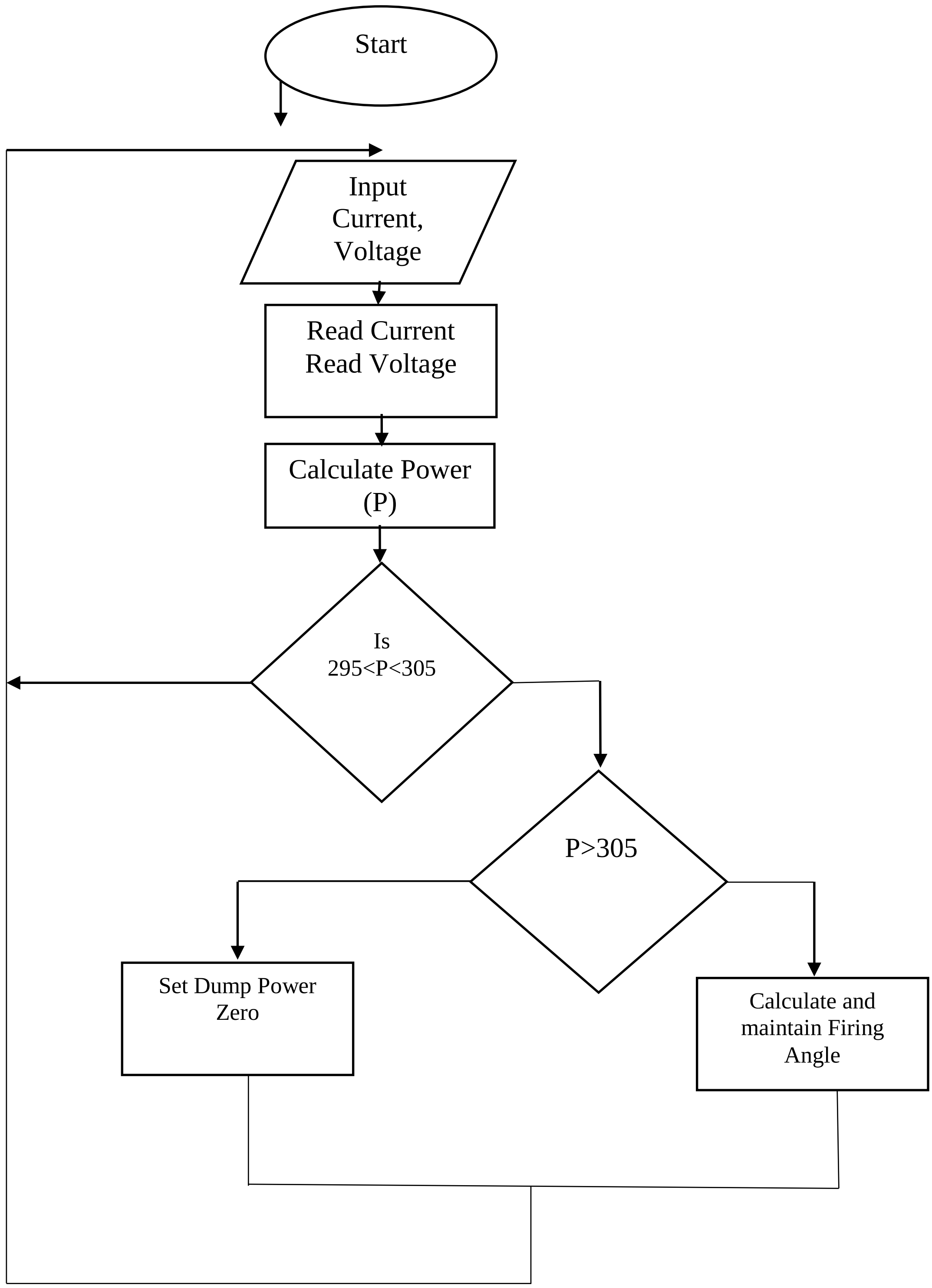

Figure 11. Triac Control Mechanism of the ELC

Kathmandu University
Journal of Science, Engineering and Technology

Giri *et. al.*, Vol. 13, No. I, October 2017, pp 20-35.

PERFORMANCE WITH NEPAL ELECTRICITY AUTHORITY SUPPLY

Electricity supply in Nepal is done by Nepal Electricity Authority (NEA). NEA has a monopoly market over distribution and transmission of electrical power in Nepal. NEA is responsible for maintaining the national grid and the performance analysis of ELC with the NEA supply will provide an optimal performance. This performance can be used for the comparison with other supply cases and studied further. The values of the current and voltage are measured with the digital power analyzer and with Wattmeter.

A. Power Profile With Resistive Load

The resistive loading offers the highest power factor available and gives a very smooth power profile as compared to capacitive or inductive loading. The power profile for the resistive loading is as shown in the figure 12.

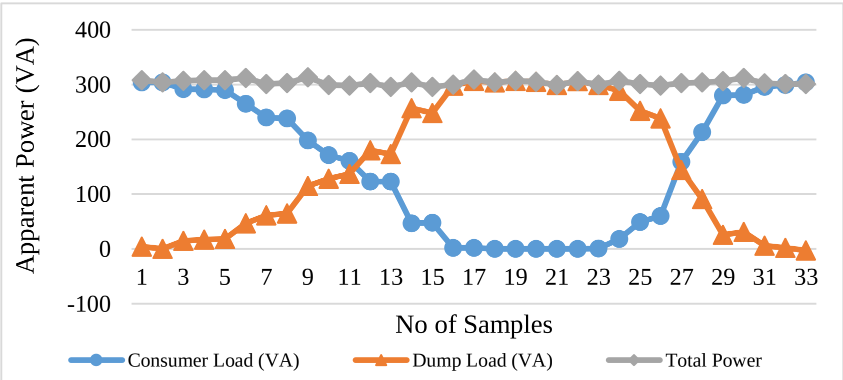

Figure 12. Power Profile with Resistive Load

Figure 12, shows that the decrease in the consumer load increases the power at the dump load and the total power is always balanced. The figure also shows the power variation at various consumer and dump loads. The variation although being very small is considered negligible.

B. System Load Profile With Inductive Load

The various inductive loads were added to the system and the performance of the system was tested. The resistive load of 785 Ohm and the inductive load having the inductance ranging from 0.146 H to 1.1179 H were used. The voltage and current profiles at Consumer side and the Dump Side for the different values of the inductance are presented in the figure 13.

Kathmandu University
Journal of Science, Engineering and Technology

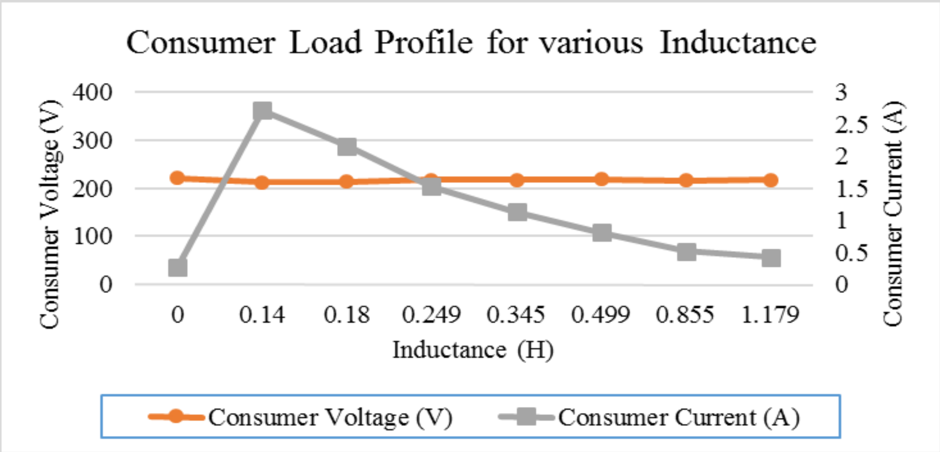

Figure 13. Consumer Load Profile with Inductive Load

Figure 13, shows that the increase in the inductive load in the consumer side decreases the current in the system.

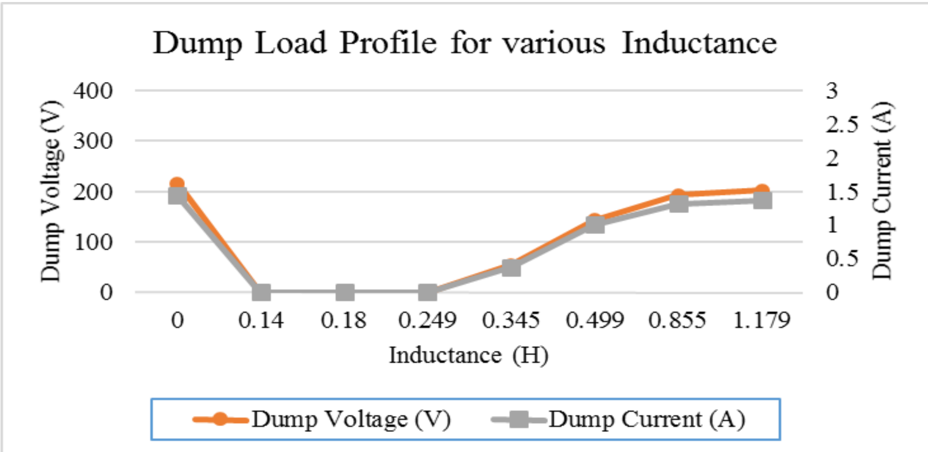

Figure 14. Dump Load Profile with Inductive Load

Figure 14, shows that the increase in the inductive load in the consumer side decreases the amount of voltage and current in the dump side. There is a gradual increase in the dump voltage and current at higher values of the inductance. This is because the increase in the inductance at the consumer side reduces the power consumed at the consumer side. So to balance the total power there is increase in the dump voltage and current.

C. System Load Profile With.Capacitive Load

The various capacitive loads were added to the system and the performance of the system was tested. The resistive load of 785 Ohm and the capacitive load having the capacitance ranging from 2.87 uF to 22.4 uF were used. The voltage and current profiles at Consumer side and the Dump Side for the different values of the capacitance are presented in the figure 15.

Giri *et. al.*, Vol. 13, No. I, October 2017, pp 20-35.

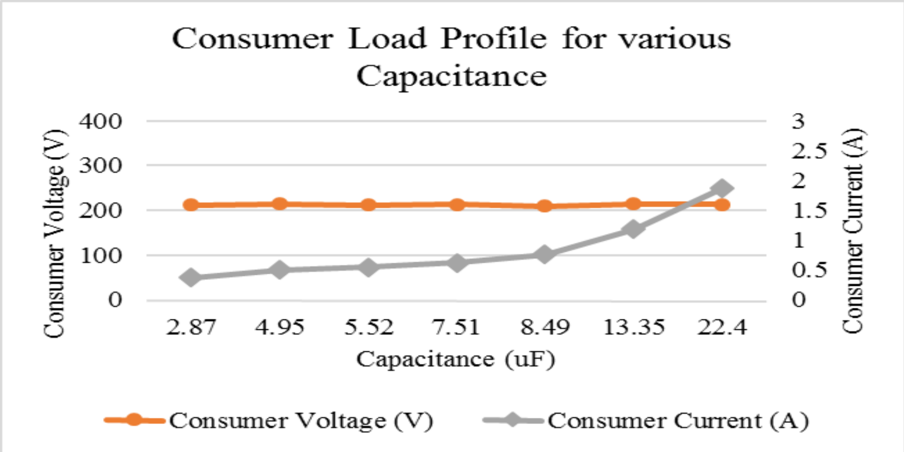

Figure 15. Consumer Load Profile with Capacitive Load

Figure 15, shows that the increase in the capacitive load in the consumer side increases the capacitive current in the system.

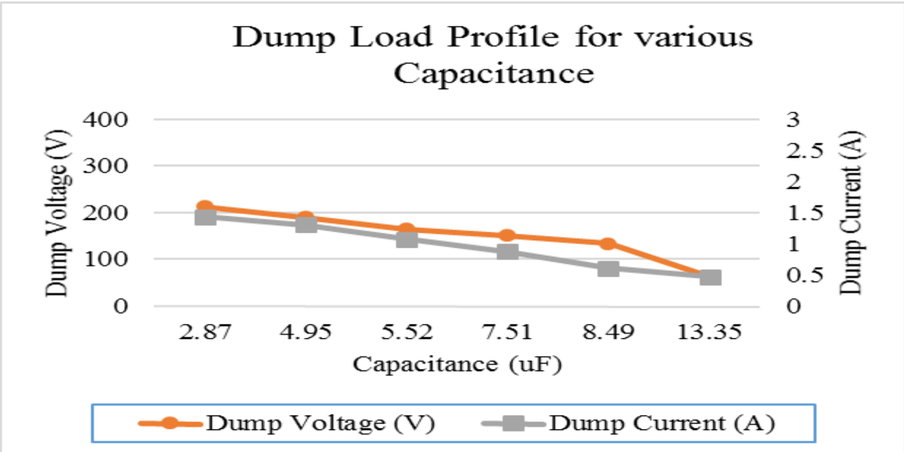

Figure 16. Dump Load profile with Capacitive Load

PERFORMANCE WITH SELF EXCITED INDUCTION GENERATOR

The power profile was obtained for various resistive, inductive and capacitive loads with Self Excited Induction Generator (SEIG). The various loadings gave various voltage, current and power profiles. The increase or decrease of the consumer load (0 VA – 200 VA) changes the power at the dump load. The different results obtained are presented.

A. Power Profile With Resistive Load

The resistive loading offers the highest power factor available and gives a very smooth power profile as compared to other loadings such as inductive and capacitive loading. The power profile for the resistive loading is as shown in the figure 17.

Giri *et. al.*, Vol. 13, No. I, October 2017, pp 20-35.

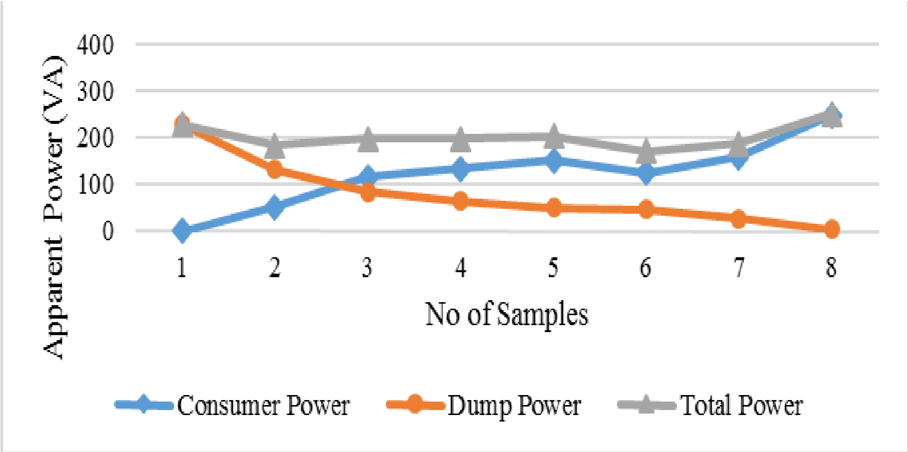

Figure 17. Power Profile with Resistive Load with SEIG

Figure 17, shows the increase in the consumer load decreasing the dump load to maintain the total power constant at every point of operation.

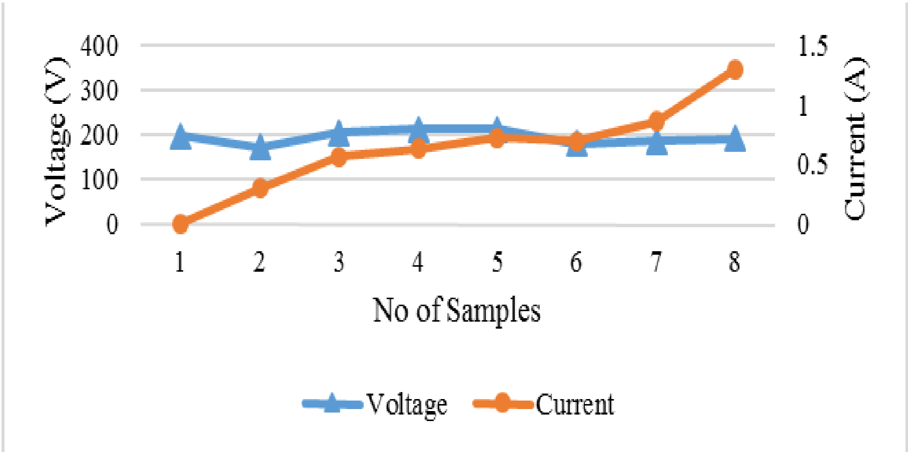

Figure 18. Consumer Load Profile with Resistive Load

Here the different resistors of decreasing value are added to the consumer load and the respective voltage and current profiles are obtained. The decrease in the resistance increases the amount of current flow in the consumer load.

Giri *et. al.*, Vol. 13, No. I, October 2017, pp 20-35.

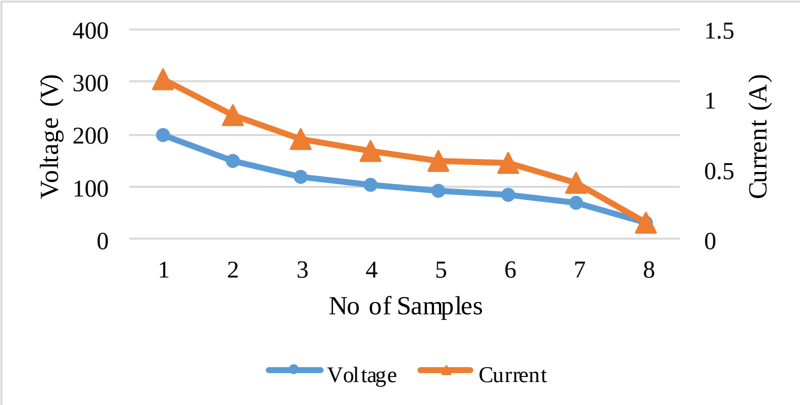

Figure 19. Dump Load Profile with Resistive Load

B. Power Profile With Capacitive Load

The different capacitive loading with fixed resistance of 1.071 K Ohm at parallel gave various current, voltage and power profiles. The power profile during capacitive loading is presented in the figure 20.

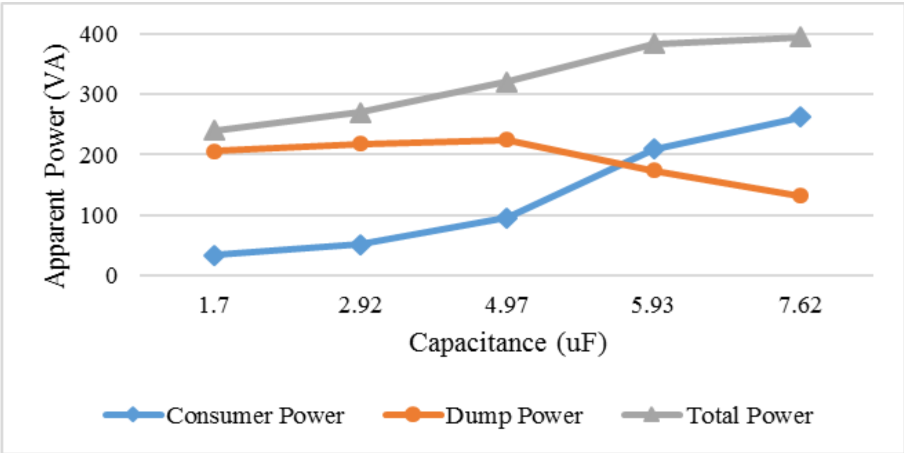

Figure 20. Power profile with Capacitive Load

Figure 20, presents the apparent power profile during various capacitive loadings. The increase in the capacitance increases the total power used by the consumer and dump load. The profile of the total power is in increasing trend and it becomes constant at about 380 VA. This is due to the increase in the system voltage due to increase of capacitance. The addition of capacitive load thus degrades the performance of the ELC.

Kathmandu University
Journal of Science, Engineering and Technology

Giri *et. al.*, Vol. 13, No. I, October 2017, pp 20-35.

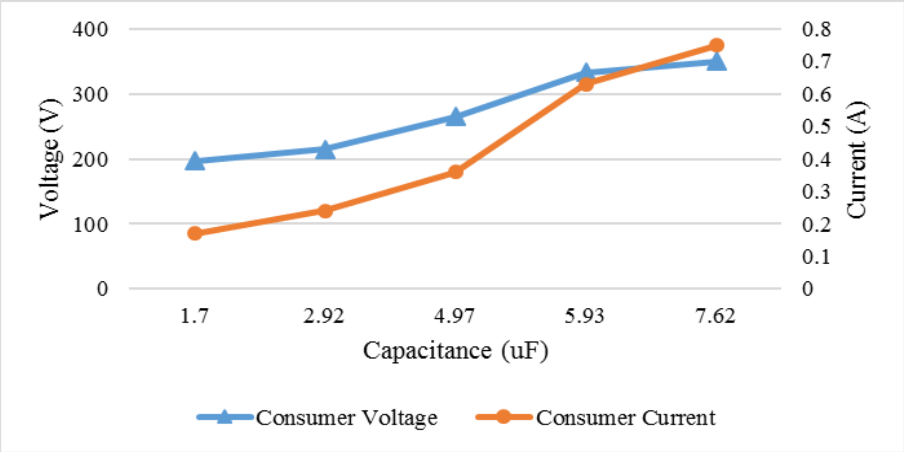

Figure 21. Consumer Load Profile with Capacitive Load

C. Power Profile During Inductive Load

The different inductive loading with fixed resistance of 1.071 K Ohm at parallel gave various current, voltage and power profiles. The power profile during inductive loading is presented in the figure 22.

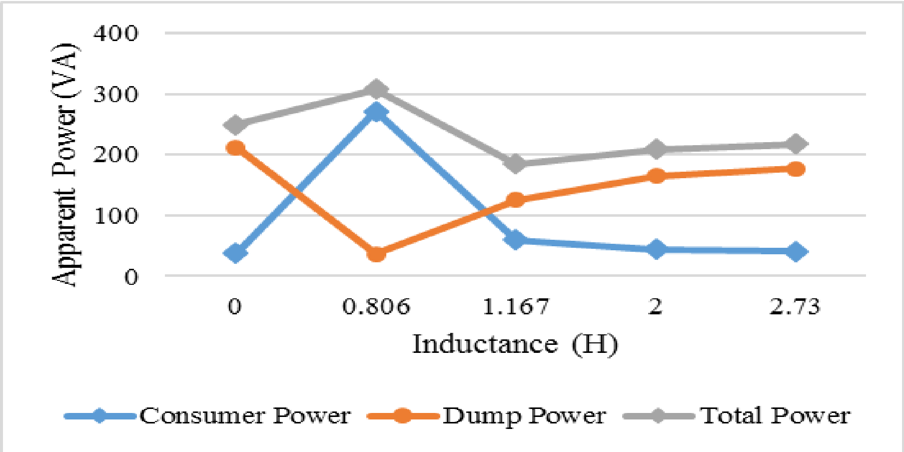

Figure 22. Power Profile with Inductive Load

CONCLUSION

The measurement of the power to control the ELC is presented in the paper. The analysis results show that the total power is constant throughout the operation of ELC. The designed ELC has good performance for the use of resistive loads. This is the best case if all the loads used in the household are of resistive type. The increase in the capacitive loadings increase the system voltage and degrade the system's performance. The increase of the inductive loading decrease the system power factor and also system voltage which degrade the system performance. Further work on power factor correction on ELC would be a good opportunity for researchers. Along with that the ELC can be used in the concept of Distributed ELC. DELC is an approach for decentralizing dump power distribution in the system with micro-hydro power as the chief power source.

Giri *et. al.*, Vol. 13, No. I, October 2017, pp 20-35.

ACKNOWLEDGMENT

The authors would like to thank their friends Mr. Narayan Shresth, Mr. Anil Wagle and Mr. Sailesh Dahal for their continuous support and encouragement throughout the course of project work.

REFERENCES

[1] Roodsari B N, Nowicki E P & Freere P, The Distributed Electronic Load Controller: A New Concept for Voltage Regulation in Microhydro Systems with Transfer of Excess Power to Households, *2013 ISES Solar World Congress. Energy Procedia*, 57 (2014), 1465–1474.

[2] Kormilo S & Robinson P, Electronic control of small hydroelectric schemes using a microcomputer, *Computers and Digital Techniques, IEEE Proceedings*, July 1984, 131 (4), 132–136.

[3] Singh B & Kasal G K, Analysis and Design of Voltage and Frequency Controllers for Isolated Asynchronous Generators in Constant Power Applications, *Power Electronics, Drives and Energy Systems, PEDES '06. International Conference*, 12-15 December 2006, 1-7,

[4] Gurung K & Freere P, Single Phase Output from 3 Phase Self Excited Induction Generators in Pico Hydro Systems, *Destination Renewables- ANZSE*, 26-29 November 2003.

[5] Rashid M H, *Power Electronics, Circuits, Devices, and Applications* (2nd Edition), Prentice-Hall of India Private Limited, India, 1996.

[6] Bimbhra P S, *Electrical Machinery*, 7th Edition, Khanna Publishers, India, 2007.